

## Vortex 'puddles' and magic vortex numbers in mesoscopic superconducting disks

This article has been downloaded from IOPscience. Please scroll down to see the full text article.

2009 J. Phys.: Conf. Ser. 150 052039

(<http://iopscience.iop.org/1742-6596/150/5/052039>)

View [the table of contents for this issue](#), or go to the [journal homepage](#) for more

Download details:

IP Address: 146.175.13.243

The article was downloaded on 05/03/2013 at 11:28

Please note that [terms and conditions apply](#).

## Vortex ‘puddles’ and magic vortex numbers in mesoscopic superconducting disks

M R Connolly<sup>1</sup>, M V Milosevic<sup>1,2</sup>, S J Bending<sup>1</sup>, J R Clem<sup>3</sup> and T Tamegai<sup>4</sup>

<sup>1</sup> Department of Physics, University of Bath - Claverton Down, Bath, BA2 7AY, UK.

<sup>2</sup> Departement Fysica, Universiteit Antwerpen - Groenenborgerlaan 171, B-2020 Antwerpen, Belgium.

<sup>3</sup> Ames Laboratory Department of Physics and Astronomy - Iowa State University, Ames, IA 50011-3160, USA.

<sup>4</sup> Department of Applied Physics, The University of Tokyo - Hongo, Bunkyo-ku, Tokyo 113-8627, Japan.

E-mail: mrc61@cam.ac.uk

**Abstract.** The magnetic properties of a superconducting disk change dramatically when its dimensions become mesoscopic. Unlike large disks, where the screening currents induced by an applied magnetic field are strong enough to force vortices to accumulate in a ‘puddle’ at the centre, in a mesoscopic disk the interaction between one of these vortices and the edge currents can be comparable to the intervortex repulsion, resulting in a destruction of the ordered triangular vortex lattice structure at the centre. Vortices instead form clusters which adopt polygonal and shell-like structures which exhibit magic number states similar to those of charged particles in a confining potential, and electrons in artificial atoms. We have fabricated mesoscopic high temperature superconducting  $\text{Bi}_2\text{Sr}_2\text{CaCu}_2\text{O}_{8+\delta}$  disks and investigated their magnetic properties using magneto-optical imaging (MOI) and high resolution scanning Hall probe microscopy (SHPM). The temperature dependence of the vortex penetration field measured using MOI is in excellent agreement with models of the thermal excitation of pancake vortices over edge barriers. The growth of the central vortex puddle has been directly imaged using SHPM and magic vortex numbers showing higher stability have been correlated with abrupt jumps in the measured local magnetisation curves.

One of the defining features of a type II superconductor in a magnetic field is the complete expulsion of magnetic flux from its interior up to the lower critical field,  $H_{c1}$ . Above this field the perfectly diamagnetic state is partially destroyed by the flux enclosed by mutually repelling microscopic vortices, which nucleate at the sample edges and penetrate to the centre where they form a ‘puddle’ of flux. It is now well established that the applied field and temperature conditions which drive a superconductor from the perfectly diamagnetic to the vortex state depend strongly on its size and shape. A particularly rich source of information relating to the influence of these two factors has been obtained from studies of disks in the mesoscopic regime where the characteristic dimensions of the sample are comparable to a single vortex (which can be either the penetration depth  $\lambda$  or the coherence length  $\xi$  depending on the material.)

Deep in the mesoscopic regime however, the screening currents interact so strongly with the vortex currents that it is invalid to assume that the stable vortex configuration within the puddle at the centre is a symmetrical triangular lattice. In mesoscopic disks, for instance, both

simulations [1] and magnetic imaging techniques [2, 3, 4] have shown that at low fields, when there are only a few vortices present, vortex clusters (regular polygons with one vortex at each vertex) are favoured over the regular triangular ordering. As the number of vortices grows, they arrange in concentric rings with each new ring forming at critical or magic vortex numbers.

The behaviour of vortex matter when the size of the disk is between the mesoscopic, where the position of each vortex has a direct influence on its superconducting state, and the macroscopic, where the only relevant parameter is the local vortex density within the vortex puddle, remains an open question. In this ‘large mesoscopic’ regime, superconductivity coexists with a large numbers of vortices, which may or may not be organized into an Abrikosov lattice. To date only a few studies have been able to access this regime experimentally. Available imaging techniques have proved to be unable to resolve individual vortices at large applied fields, while local magnetisation curves do not generally exhibit discontinuities that can be directly associated with the transitions between different fluxoid states seen in smaller mesoscopic disks [5]. In the absence of strong features related to individual vortices, the quasi-continuous magnetisation curves and flux profiles of large superconducting disks can be rather well described by classical continuum electromagnetism [6, 7].

In this work we have used high spatial resolution scanning Hall probe microscopy (SHPM) and magneto-optical imaging (MOI) to observe the stray diamagnetic and vortex fields at the surface of arrays of large mesoscopic high temperature superconducting  $\text{Bi}_2\text{Sr}_2\text{CaCu}_2\text{O}_{8+\delta}$  (BSCCO) disks fabricated on the surface of a platelet single crystal. The as-grown BSCCO single crystal ( $T_c \approx 91$  K, dimensions  $\approx 2.5$  mm  $\times$  2 mm  $\times$  100  $\mu\text{m}$ ) was cleaved and arrays of disks were patterned into the surface to a depth of 300 nm using photolithography and Argon ion beam milling. A typical region of the array, shown in Fig. 1, consists of 4 disks with nominal diameters of 5  $\mu\text{m}$ , 10  $\mu\text{m}$ , 15  $\mu\text{m}$ , and 20  $\mu\text{m}$  arranged around a 40  $\mu\text{m}$   $\times$  40  $\mu\text{m}$  square unit cell with lattice constants inclined at approximately 45° to the crystallographic  $a$ -axis of the crystal.

The disk array was initially cooled below  $T_c$  and imaged using a low-temperature magneto-

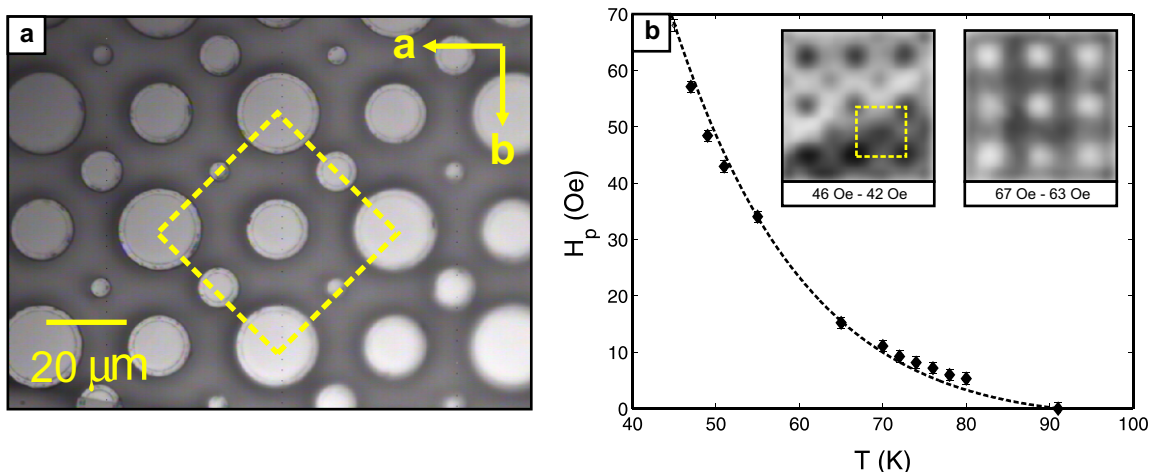


**Figure 1.** (a) Optical micrograph of the disk array showing the orientation of the unit cell 40  $\mu\text{m}$   $\times$  40  $\mu\text{m}$  square unit cell (dashed outline) and the directions of the crystallographic  $a$ - and  $b$ -axis. (b) MO difference images below (left) and above (right) the penetration field  $H_p$  of the 20  $\mu\text{m}$  disk [dashed outline has the same meaning as in (a).] (Main plot) Measured temperature dependence of the penetration field (solid diamonds) and fit (dashed line) to the data using the model for the Bean-Livingston surface barrier [8, 9].

optical imaging system based on a cryocooler (details of the system can be found in Ref. [10].) Figure 1(b) shows two MO difference images, i.e., images obtained by subtracting two raw images, taken in increasing applied fields after cooling the sample to  $T = 45$  K. As anticipated, the change in the distribution of flux for the low fields is strongly modulated by the presence of the disks. In particular, the intensity in the interstitial regions increases while the intensity over the unpenetrated disks remains low in comparison. At slightly higher fields the opposite behaviour is observed and the disks exhibit the strongest positive change in flux. (Clearly, in Fig. 1 this is only happening in the  $20 \mu\text{m}$  disks, and it is not until a somewhat higher field that the smaller disks begin to be penetrated.) By systematically analysing difference images at various temperatures we were able to establish the temperature dependence of the penetration field,  $H_p(T)$ , when flux first forms a central puddle in the  $20 \mu\text{m}$  diameter disks. These data are plotted in Fig. 1(b). The experimental form of  $H_p(T)$  shows a rapid decay with increasing temperature, in good agreement with models based on the thermal activation of vortices over surface barriers (see, for instance, Ref. [8] and [9].)

In order to analyse the formation of the vortex puddle in greater detail, in our next experiments the array was cooled to  $T = 77$  K and high spatial resolution SHPM images were captured at regular (increasing) field intervals. Again, difference images are used in this study to enhance the contrast due to small numbers of penetrating vortices which cannot be resolved in raw SHPM images. Fig. 2(a)-(b) shows that, as expected, for fields just above the penetration field  $H_p$ , a puddle of flux is formed which expands with increasing applied field as vortices accumulate at the centre. In Fig. 2(b) we present the experimentally measured local magnetisation captured in decreasing field with the SHPM Hall sensor parked at the centre of this disk. Despite the loss of single vortex resolution in the SHPM images, we observe striking

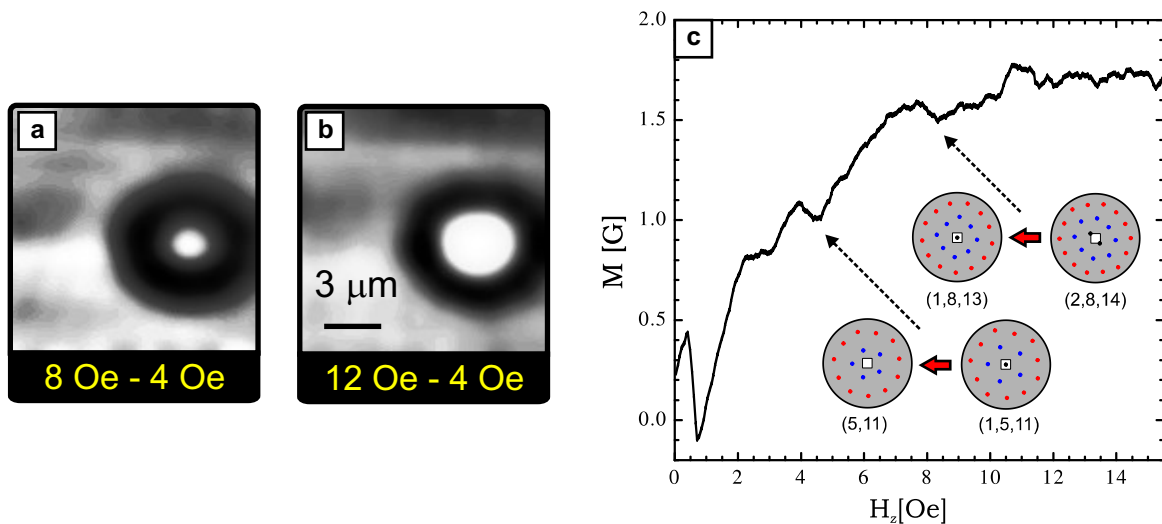


**Figure 2.** (a),(b) Typical 77 K SHPM difference images ( $13 \mu\text{m} \times 13 \mu\text{m}$ ) showing the growth of the vortex puddle with increasing applied field. (The disk is unpenetrated in the reference field  $H_z = 4$  Oe.) (c) Experimentally obtained local  $M(H_z)$  curves for decreasing fields. The configurations shown in inset are results of calculations based on molecular dynamics simulations and illustrate the transitions which occur at two fields where there is a pronounced feature in the magnetisation. The numbers in brackets beneath each configuration refer to the number of vortices in each shell and the white square represents the size and location of the Hall probe.

features in this curve which can be directly correlated to the underlying configuration of vortices. It is already well known that vortices in mesoscopic disks tend to form concentric shells [1]. As vortices leave the disk in decreasing fields, it is always the case that the innermost shell collapses first, at which point the last central vortex is integrated into the other shells. Consequently, for a Hall probe placed above the centre of the disk, there is always a sharp increase in the measured magnetisation when a shell collapses. By performing molecular dynamics simulations based on the theory outlined in Ref. [11], we are able to show that the jumps in the curve of Fig. 2(b) can be directly correlated with the transitions involving the collapse of the innermost shell [for illustration, see the calculated configurations (1, 5, 11)  $\rightarrow$  (5, 11) in Fig. 2(b)] or transitions between multi-vortex structures within the core of the shell structure [see inset configurations for  $H_z \approx 8$  Oe in Fig. 1(b).]

In conclusion, we have presented the first experimental study of large mesoscopic superconductors (high- $T_c$  disks) which has been able to investigate the penetration and configurations of vortices in large mesoscopic disks. In disks of 20  $\mu\text{m}$  diameter we have used MO imaging to measure the penetration field and find excellent agreement with models for the thermal activation of vortices over surface barriers. Using high spatial resolution Hall probe magnetometry we have shown that large mesoscopic disks continue to exhibit discreteness through characteristic features in the local  $M(H_z)$  curves. These measurements, in combination with numerical simulations, allow us to identify the magnetic signatures of individual vortices penetrating the centre of the disk and the assembly process of vortices into different shell formations.

### Acknowledgments

This work was supported by EPSRC-UK under grant No. GR/D034264/1 and the Royal Society through an International Joint Project No. 2005/R1. M.V.M. is a Marie-Curie Intra-European Fellow at the University of Bath. J.R.C. acknowledges support by the Department of Energy - Basic Energy Sciences under Contract No. DE-AC02-07CH11358. T.T. acknowledges support from JSPS bilateral cooperative program.

### References

- [1] Schweigert V A, Peeters F M and Deo P S 1998 *Phys. Rev. Lett.* **81** 2783
- [2] Grigorieva I, Escoffier W, Richardson J, LY Vinnikov S and Oboznov J 2006 *Phys. Rev. Lett.* **96** 077005
- [3] Nishio T, Okayasu S, Suzuki J and Kadowaki K 2004 *Physica C* **379-384** 412-414
- [4] Nishio T, Chen Q, Gillijns W, Keyser K D, Vervaeke K and Moshchalkov V V 2008 *Phys. Rev. B* **77** 012502
- [5] Geim A, Dubonos S, Lok J, Henini M and Maan J 1998 *Nature* **396** 144
- [6] Benkraouda M and Clem J R 1996 *Phys. Rev. B* **53** 5716
- [7] Zeldov E, Larkin A I, Geshkenbein V B, M Konczykowski D M, Khaykovich B, Vinokur V M and Shtrikman H 1994 *Phys. Rev. Lett.* **73** 1428
- [8] Burlachkov L, Geshkenbein V B, Koshelev A E, Larkin A I and Vinokur V M 1994 *Phys. Rev. B* **50** R16770
- [9] Kopylov V N, Koshelev A E and Schegolev I F 1990 *Physica C* **170** 291-297
- [10] Tamegai T, Matsui M, Yasugaki M, Tokunaga Y and Tokunaga M 2004 *Magneto-optical imaging: Vol. 142 of NATO Science Series II: Mathematics, Physics, and Chemistry* (Kluwer Academic Publishers)
- [11] Cabral L R E, Baelus B J and Peeters F M 2004 *Phys. Rev. B* **70** 144523